Tukka AA *et al.* (2025)
Nova Geodesia 5(1):252
Research Article

# Enhanced geoid modelling in local geodetic networks: Comparative analysis of Least Squares Collocation techniques

Apollos A. TUKKA*, Timothy O. IDOWU, Herbert TATA

*Federal University of Technology Akure (FUTA), School of Environmental Technology, Department of Surveying and Geoinformatics, Ondo State, Nigeria; aatukka@futa.edu.ng (*corresponding author); toidowu@futa.edu.ng; htata@futa.edu.ng*

## Abstract

The geoid is an equipotential surface of the Earth's gravity field that closely approximates mean sea level in a least-squares sense. Meanwhile, this study aims to enhance local geoid modeling by comparing the Stationary (SLSC) and Non-Stationary Least Squares Collocation (NSLSC) techniques in Akure South and Gombe, Nigeria. Performance evaluation of the techniques, including comparison of SLSC and NSLSC approaches using three (Gaussian, Exponential, and Matern) covariance models and statistical (MANOVA) analysis, was carried out. In the Akure study area, Matern covariance model, though requiring longer processing time, has proved to be the best-fit (optimum) model for the application of SLSC and NSLSC techniques with standard deviations of 1.711825 m and 1.711782 m respectively. Also, using the GGM dataset for both approaches, the standard deviations for both approaches yielded 1.538476 m and 1.538454 m respectively. Furthermore, using the DEM dataset for both approaches, the standard deviations for both approaches yielded 0.943200 m and 0.943198 m respectively. However, in the Gombe study area, using terrestrial datasets, the Gaussian function proved to be the best-fit (optimum) model yielding the standard deviations of 0.352219 m and 0.352564 m for SLSC and NSLSC techniques, respectively. The results obtained from the GGM datasets yielded standard deviations of 0.340943 m and 0.338443 m for the SLSC and NSLSC techniques, respectively, while the DEM datasets produced standard deviations of 0.352285 m and 0.352496 m for the two techniques, respectively. The findings suggest that NSLSC is better suited for geoid determination in mountainous terrains like Akure South due to its flexibility, while SLSC is computationally more efficient for gently rolling terrains such as Gombe.

***Keywords:*** covariance models; geoidal height; least square collocation; nonstationary; stationary; varied terrain

## Introduction

The geoid is an equipotential surface of the Earth's gravity field that best fits the mean sea level in the least-squares sense (Marchenko *et al.*, 2002). In physical geodesy, the geoid is a reference surface for orthometric height determination, typically derived through spirit leveling (Heiskanen and Moritz, 1967). With advancements in Global Navigation Satellite Systems (GNSS), geodetic heights can be directly determined relative to the reference ellipsoid, necessitating an accurate geoid model for conversion to orthometric heights

*Received: 08 Dec 2024. Received in revised form: 18 Feb 2025. Accepted: 24 Feb 2025. Published online: 02 Mar 2025.*

(Saadon *et al.*, 2021). Geoid determination methods include GPS/leveling, satellite gravimetry, and gravimetric approaches, among others (Barthelmes, 2018; Goli *et al.*, 2019). This study focuses on a gravimetric geoid modeling technique utilizing Least Squares Collocation (LSC), which estimates missing gravity data by predicting spatial correlations based on covariance functions. When using the traditional Stokes's integral function to represent gravity field-dependent parameters, the gravimetric geoid modeling approach based on Stokes's method requires gravity observations across a dense and continuous network of stations within the study area. However, terrestrial gravity measurements have historically been collected at sparse points (Telford *et al.*, 1990; Torge, 2001). Logistical, economic, and accessibility constraints often limit data collection at specific locations, making it impractical to achieve the required continuous coverage. After the gravity values are measured at selected discrete points, the unobserved locations are estimated using appropriate prediction techniques such as the Least Squares Collocation (LSC) (Ono *et al.*, 2017; Odumosu *et al.*, 2021).

The Least Squares Collocation (LSC) method has become a widely used technique in geoid modeling, offering a significant advantage over other methods by providing solutions for determining points that cannot be directly observed (Ramouz *et al.*, 2019; Timilsina *et al.*, 2021; Al-Ajami *et al.*, 2022).

In mathematical geodesy, the Least Squares Collocation (LSC) technique serves as an estimation method to provide numerical solutions for geodetic problems relying on the structure of the covariance function to account for spatial dependence in observed datasets, thus, enabling accurate numerical solutions for geodetic issues within a given locality (Krarup, 1969; Torge, 2001; Idowu, 2006; Darbeheshti and Featherstone, 2009; Ono *et al.*, 2017). Meanwhile, recent studies (Darbeheshti and Featherstone, 2010) revealed that geoid models can be determined using what is referred to herein as the Stationary Least Square Collocation (SLSC) and Nonstationary Least Square Collocation (NSLSC) techniques. The notion of SLSC is commonly utilized in classical geodesy. This notion is founded on the concepts that the observed dataset's mean remains constant throughout the research region and that the covariance function utilized is isotropic; meaning it has a uniform shape in every direction. Additionally, it is dependent only on the separation (correlation) distances between the observations (Meissi, 1971; Moritz, 1978; Knudsen, 2005; Risser and Calder, 2015).

According to Risser and Calder (2015), the SLSC concept assumes an isotropic structured covariance function to capture spatial variability, meaning that, the statistical properties of the gravity field data remain constant across the study area. When used in a case study in western Australia, the SLSC approach proves to be computationally efficient but failed in regions with significant terrain variations (Darbeheshti and Featherstone, 2010). Interestingly, the NSLSC approach was discovered through further review and is thought to be a superior substitute method currently employed in the field of spatial sciences, including geodetic research (Darbeheshti and Featherstone, 2010). Here the approach allows for a non-uniform spatial correlation covariance structure evaluation, making it suitable for complex terrains where gravity variations are non-uniform (Darbeheshti and Featherstone, 2009). However, regardless of which computation method is selected, geodetic scientists typically must undergo time-consuming mathematical procedures involving complex systems of equations, matrix formulations and inversions, to estimate the gravity field parameters needed for a geoid determination. This makes the LSC technique computationally intensive, posing challenges in large-scale geoid modeling projects (Krarup, 1969; Meissi, 1971; Moritz, 1978; Knudsen, 2005; Risser and Calder, 2015; Ono *et al.*, 2017).

Despite utilizing the LSC in previous studies (Tscherning and Rapp, 1974; Goad *et al.*, 1984; Knudsen, 1987; Milbert, 1992; Kenyon and Pavlis, 1997; Collier *et al.*, 1998; Featherstone, 1998; Kenyon, 1998; Tscherning *et al.*, 1998; Abd-Elmotaal, 1998; Denker *et al.*, 2000; Tscherning, 2001; Marchenko *et al.*, 2002; Zhang and Featherstone, 2004; Kwon *et al.*, 2005; You and Hwang, 2006; Alberts *et al.*, 2007; Maggi *et al.*, 2007; Marti, 2007; Lyszkowicz, 2010), for geoid determination, the comparative performance of stationary and non-stationary covariance models within Nigeria's diverse topographic settings remains largely unexplored. Hence, this study evaluates the effectiveness of SLSC and NSLSC techniques in geoid modeling across Akure (a mountainous terrain) and Gombe (a gently rolling terrain); with the view to determine the most suitable

technique based on these terrain characteristics. This study represents a significant advancement in local gravimetric geoid determination by employing both Stationary and Non-Stationary Least Squares Collocation (SLSC and NSLSC) approaches across the two distinct terrain types. Unlike traditional methods of LSC that primarily assume stationarity in covariance modeling alone, this research investigates the effects of incorporating the non-stationary structured covariance models to enhance flexibility to complex gravity field variations. While the NSLSC offers a superior geoid estimation potential, the study also explores the computational efficiency of these approaches in identifying a trade-off between accuracy and processing time. By combining this advanced statistical modeling with high-resolution datasets from existing gravity field models, and varied covariance structures, this research aimed at enhancing the precision and applicability of local gravimetric geoid models beyond the scope of previous works.

The Matérn covariance model, as highlighted by Meissi (1971), Higdon *et al.* (1999), Paciorek (2003), and Risser and Calder, (2015), enables spatial correlation modeling, enhancing geoid precision via adaptable and continuous spatial representation. However, its computational complexity poses challenges, particularly for large datasets (Paciorek and Schervish, 2006). The use of the Matérn model mostly makes direct matrix inversion computation infeasible for large datasets; were the issue of storage and memory demand, alongside the increase in covariance matrix size, further complicates its implementation. Furthermore, parameter estimation requires optimizing variance and correlation length, which adds to its computational cost. To address these challenges, various approaches such as stochastic estimation techniques, including Monte Carlo methods and approximate likelihood functions, among others, have been applied to mitigate its computational burden (Higdon *et al.*, 1999). Hence, the foregoing studies suggest that, these trade-offs between accuracy and computational efficiency must be carefully considered when applying the different types of covariance model in geoid modeling.

Therefore, by systematically comparing Gaussian, Exponential, and Matérn covariance structures, the study provides new insights into optimizing geoid estimation accuracy, while balancing computational efficiency. According to Tata (2024), "The general insight to be gained from the gravimetric geoid model can contribute to geophysical studies within any given locality, by providing understanding on the subsurface geological structures mostly extracted from the long wavelength component of the gravity anomaly known as regional anomalies, and tectonic processes which can further aid in assessing seismic hazards, groundwater movement, and other geological phenomena".

*Theoretical Concept*

This study is hitched on the theoretical concept of gravimetric surveying, gravimetric geoid, least square collocation techniques, and its mathematical formulation for the determination of gravimetric geoid based on the Molodensky approach.

*Gravimetric Surveying*

The basis on which gravity surveying depends is found in the concept of equating two Newton's laws (Reynolds, 1998):

$$F=\frac{KmM}{r^2} \quad (1)$$

$$F=mg \quad (2)$$

Combining equations (1) and (2) gives:

$$g=\frac{KM}{r^2} \quad (3)$$

*Where* F represents the gravitational force between two objects; K is the gravitational constant, a universal constant approximately equal to $6.67430 \times 10^{-11} m^3 kg^{-1} s^{-2}$; m and M are the masses of the two objects; r is the distance between the centers of the masses m and M.

*Gravimetric Geoid*

Gravimetric geoid modeling relies on the evaluation of the concept of gravity anomaly, obtained from reduced and normal gravity values of observation stations, given as (Hakenen and Moritz, 1967):

$$\Delta_g = g_r - \gamma \quad (4)$$

Where $\Delta_g$ = Gravity anomaly; $g_r$ = Reduced gravity; and $\gamma$ = Normal gravity (from a referenced Ellipsoid)

*Least Squares Collocation:*

The concept of the LSC technique is based on a functional and stochastic model represented by Equation (5) (Ayeni,1981), where observations are explicitly written in terms of the unknown parameters as:

$$L^a = f(x^a), \;\; P_l = \sigma_o^2 C_l^{-1} \quad (5)$$

Its concept combines least squares adjustment to obtain parameters (X), least squares filtering of error (V) and least squares prediction of signals (S) using observed quantities (l). As in Rapp (1986), the ultimate generalization and the minimum principle of the linear least squares collocation model are respectively given as (6) and (7).as:

$$l = AX + S + V \quad (6)$$

$$S^T C_{sl}^{-1} R + V^T C_{VV}^{-1} V = Minimum \quad (7)$$

Where: $C_{sl}$= Covariance function between observations and signals $C_{VV}$= Covariance matrix between residuals of observations; A = $\frac{\partial L}{\partial X}$ in mxn matrix of coefficients; The superscript T indicates the transpose of a vector and/or matrix.

Generally, the covariance function reflects the behavior of the anomalous field, describing the magnitude of variation and roughness, which characterizes the statistical correlation between two or more quantities within the anomalous field at different point locations (Guimarães *et al.*, 2014).

*Role of Covariance Function in LSC*

In the context of the LSC technique, the covariance function governs the weighting of observations for spatial determination. Schwarz and LaChapelle (1980) and Idowu (2008) recommended that the covariance function should be simple, analytical, isotropic, and homogeneous. The requirements of isotropy and homogeneity mean that the covariance function must be invariant under rotation and translation, implying a stationary, structured covariance function (Risser and Calder 2017). While these assumptions facilitate the geoid determination process, they may not always hold across all regions because there are different types underground mass distribution, and also there exist several types of stationary and nonstationary structured covariance functions, such as Gaussian, exponential, and Matérn (Risser and Calder, 2015), that can be used, as shown in Table 1. The table summarizes three types of covariance function models, by comparing their stationary and non-stationary formulations for spatial correlation modeling.

**Table 1.** Types of Covariance Function Models (s)

| Model | Stationary Model | Non-Stationary Model |
|---|---|---|
| Gaussian | $C_0\, e - (\frac{r2}{d2})$ | $C(S_i, S_j) = C_0 * [\Sigma_i]^{\frac{1}{4}} * [\Sigma_j]^{\frac{1}{4}} * \left\lvert \frac{[\Sigma_i] + [\Sigma_j]}{2} \right\rvert^{-\frac{1}{2}} * \exp^{-Q_{ij}}$ |
| Exponential | $C_0 \left(1 + \frac{r}{D}\right) e^{-r/D}$ | $C(S_i, S_j) = C_0 * [\Sigma_i]^{\frac{1}{4}} * [\Sigma_j]^{\frac{1}{4}} * \left\lvert \frac{[\Sigma_i] + [\Sigma_j]}{2} \right\rvert^{-\frac{1}{2}} * (1 + Q_{ij}) \exp^{-Q_{ij}}$ |
| Matérn | $C_0 \left(1 + \frac{r}{D} + \frac{r^2}{3D^2}\right) e^{-r/D}$ | $C(S_i, S_j) = C_0 * [\Sigma_i]^{\frac{1}{4}} * [\Sigma_j]^{\frac{1}{4}} * \left\lvert \frac{[\Sigma_i] + [\Sigma_j]}{2} \right\rvert^{-\frac{1}{2}} * (1 + Q_{ij} + \frac{Q_{ij}^2}{3}) \exp^{-Q_{ij}}$ |

Despite the availability of these covariance models cited above among others, the issue of local gravimetric geoid determination within Nigeria has not been resolved through these SLSC and NSLSC covariance function models. By addressing this research gap, the study will significantly enhance our understanding of the practical implications of the Gaussian, Exponential, and Matérn covariance Models for estimating local gravimetric geoid using the Stationary and Nonstationary structured LSC approach and underscore their relevance across the selected terrain types used in the study.

*Geoid Estimation based on LSC-Molodensky Approach*

In this study, the geoidal undulation (N) at any point P ($\phi, \lambda$) on the Earth's surface can be computed by evaluation of the Molodensky's model given by Equation (8 to 12) (Ramouz *et al*, 2019; Timilsina *et al.*, 2021; Al-Ajami *et al.*, 2022):

$$N = \xi + \frac{\Delta_{g_B}}{\bar{\Upsilon}} H \tag{8}$$

$$\xi = \xi\, GGM + \xi\, RTM + \xi_{res} \tag{9}$$

$$\xi_{res}(P) = \frac{T_{res}(P)}{\gamma(P)} \tag{10}$$

$$T_{res}(P_i) = C_{T_{res}\,\Delta g_{res}(P_i\,j)} * C^{-1}_{\Delta g_{res}\,\Delta g_{res}(P_i\,j)} * \Delta g_{res}(P_i) \tag{11}$$

$$\Delta g_{res}(P_i) = \Delta g_{Obs}(P_i) - \Delta g_{GGM}(P_i) \tag{12}$$

Where: $\xi$ is the undulation of the quasi-geoid; $\xi\, GGM$ represents the long wavelength component computed from Global Geopotential Models (GGM); $\xi\, RTM$ represents the short wavelengths component of the height anomalies caused by the topography of the area; $\xi_{res}(P)$ is the residual height anomaly; $T_{res}(P_i)$ is the residual gravity field to be obtained from the least-squares collocation method; $C_{T_{res}\,\Delta g_{res}(P_i\,j)}$ represents the matrix of the cross-covariance between the residual gravity field (Tres) and the residual gravity anomalies(Δgres); $C^{-1}_{\Delta g_{res}\,\Delta g_{res}(P_i\,j)}$ represents the auto-covariance matrix of the residual gravity anomalies; $\Delta g_{res}(P_i)$ are the residual gravity anomalies; H is the station elevation; $\Delta_{g_B}$ incomplete Bouguer anomalies; $\bar{\Upsilon}$ is the mean normal gravity, and N is the station geoidal undulation based on Molodenskys' approach (Al-Ajami *et al.*, 2022).

According to Dagogo *et al.* (2014), "solving Molodensky's problem yields the quasi-geoid, which, if adopted, deviates from the geoid by only a few centimeters. Hence, Molodensky's algorithm is useful not only for defining the Earth's physical surface but also for determining the geoid". Therefore, the application of the LSC, incorporating SLSC and NSLS covariance models alongside the Molodensky's approach remains underexplored in Nigeria's diverse topographies, leaving a critical gap in geoid modeling accuracy assessment. Hence, this study aims at the integration of these advanced geostatistical methodologies with the view to ensuring a reliable representation of the geoidal surface within the study area, which will contribute to an improved height system realization and geodetic applications within Nigeria.

## Materials and Methods

*Study Area*

Due to the availability of data and the need to capture differences in the properties of the gravitational field, the study focuses on two geodetically significant locations within Nigeria. Akure South (Ondo State) and Gombe State were selected due to their contrasting topographic features as shown in Figure 1(a) and 1(b). Akure is located within the rainforest belt of Nigeria and lies between latitude 07° 14′ 50 ″N and 07° 18′ 30 ″N and longitudes 05° 08′ 40 ″E and 05° 12′ 05 ″E, in southwestern Nigeria; it is characterized by rugged terrain, steep slopes, and significant elevation variations, representing a challenging environment for geoid modeling. Gombe, in contrast, exhibits a relatively smooth and gently rolling terrain, spanning from Latitude

of 10° 14′ 22.5 ′N to 10° 59′ 18.8 ″N and Longitude $10^0$ 08′ 50.1″E to $11^0$ 07′ 15.3″E (Idowu, 2006; Oladapo and Afuda, 2016).

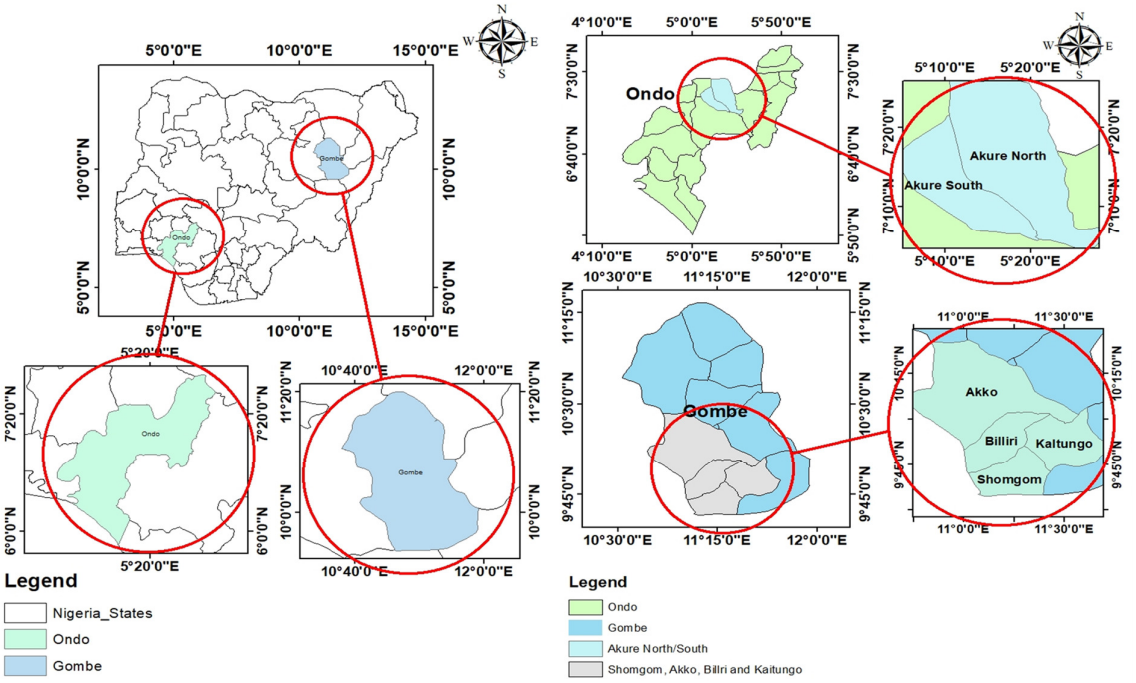


**Figure 1. (a)** Ondo and Gombe states in the national setting; **(b)** Locational map of study areas

The choice of Akure and Gombe as study areas is motivated by their distinct topographic characteristics, which effectively represent part of the diversity of terrain types in Nigeria. Akure, located in the southwestern region of Nigeria, is characterized by a predominantly mountainous and undulating terrain, with significant variations in elevation. The presence of rugged topography, steep slopes, and variable gravity anomalies makes it an ideal setting to assess the performance of geoid modeling techniques in complex landscapes. This region serves as a testbed for evaluating how the Stationary and Nonstationary Least Squares Collocation technique can capture spatial variability in geoid undulations, given the non-homogeneous nature of the gravity field.

On the other hand, Gombe, situated in the northeastern part of Nigeria features a gently rolling terrain with relatively smooth elevation changes, that transformed into savannah and semi-arid regions. The contrast between Akure's rugged terrain and Gombe's more uniform landscape allows for a comprehensive evaluation of both stationary and nonstationary covariance approaches in geoid modeling.

By selecting these two regions, the study aims to ensure that the results are applicable across these Nigeria's diverse geophysical environments. This diversity is crucial in validating the use of these different covariance models and Least Squares Collocation techniques under these varied topographic conditions. Ultimately, the selection of Akure and Gombe as test sites would strengthen the study's contribution to improving local geoid model estimation by providing insight that can be effectively applied within similar terrain types across Nigeria and elsewhere.

*Method*

The study's methodology is structured into phases involving data collection, quality evaluation, presentation, and processing to estimate the local gravimetric geoid. Here, secondary datasets were primarily used, these included: geopotential models (EGM2008, SGG-UGM-2, and XGM2019e_2159), and terrestrial gravity data from the Gombe and Akure states. Similarly, Digital Elevation Models (ALOS-PALSAR, ASTER, and TANDEM) datasets were sourced from ICGEM and USGS, these are reputable institutions that provide

relatively stable gravity field representations that are crucial for geoid modeling. In this study, the data processing follows three phases of processing strategies, using the Least Squares Collocation (LSC) technique. Phase one (1) includes: gravity reductions and terrain effect estimations. Phase two (2) involves: fitting spatially-varying models for residual gravity field estimation using Gaussian, Exponential, and Matérn covariance models. The final phase (3) integrates these contributions to compute the complete quasi-geoid and geoidal undulations using the Molodensky approach. All computations were performed in an R coding environment, by adapting and modifying the Convo-SPAT package (Risser and Calder, 2015) for geodetic applications, to ensure precise evaluation of both the stationary and non-stationary covariance functions.

*Data Quality*

The terrestrial gravity data, geopotential and digital elevation models used for the computations of local geoids for the two terrains are of high quality based on the information obtained from the sources of the data.

*Data Presentation: Data Used and Sources*

Several types of secondary datasets were utilized in this study to achieve the aim of the study. The sample data types used herein for the study are presented. Tables 2 to 8 present summarily these sample datasets and their sources collected from the Akure and Gombe study areas, respectively. Table 2 presents a summary of the rectangular coordinates (Easting and Northing) and their sources from fieldwork in Akure and Gombe, with Akure having 59 points (Tata *et al.*, 2019) and Gombe having 330 points (Idowu, 2006).

**Table 2.** Summary of rectangular coordinates and sources

| Region(s) | Parameters (coordinates) | No of points | Max. (m) | Min. (m) | Source |
|---|---|---|---|---|---|
| Akure | Easting | 59 | 746666.76 | 737010.22 | Tata *et al.* (2019) |
| | Northings | 59 | 804857.74 | 793477.67 | |
| Gombe | Easting | 330 | 697203.1 | 656649.7 | Idowu (2006) |
| | Northings | 330 | 122242.1 | 110467.8 | |

Table 3 provides latitude coordinate summaries for Akure and Gombe, showing Akure's latitude ranging from 7.174° to 7.277° and Gombe's from 9.989° to 11.054°, sourced from Tata *et al.* (2019), Idowu (2006), and SNEPCO (1995).

**Table 3.** Summary of latitude coordinates and sources from Akure and Gombe fieldwork

| Region(s) | Parameters (coordinates) | No of points | Max. (D. Deg) | Min (D. Deg) | Source |
|---|---|---|---|---|---|
| Akure | Latitude | 59 | 7.277 | 7.174 | Tata *et al.* (2019) |
| Gombe | Latitude | 330 | 11.054 | 9.989 | Idowu (2006); SNEPCO (1995) |

Table 4 summarizes the terrestrial gravity data, indicating a near-constant mean gravity value of 9.781 mGal in Akure, while Gombe shows more variation with values ranging from 9.731 mGal to 9.781 mGal, sourced from Tata *et al.*, (2019), Idowu (2006), and SNEPCO (1995).

**Table 4.** Summary of Terrestrial gravity and sources

| Parameters Terrestrial gravity | No of points | Max. (mGal) | Min. (mGal) | Mean (mGal) | Std. dev (mGal) | Source |
|---|---|---|---|---|---|---|
| Akure | 59 | 9.781 | 9.781 | 9.781 | 4.709E-05 | Tata *et al.* (2019) |
| Gombe | 330 | 9.781 | 9.731 | 9.780 | 8.988 | Idowu (2006); SNEPCO (1995) |

Table 5 details the GGM-derived gravity anomalies for Akure, where EGM2008 reports the highest anomaly values (50.536 mGal max), while SGG-UGM and XGM2019e present lower variations in both gravity and height, sourced from ICGEM (2023).

**Table 5.** Summary of GGM-Gravity Anomaly and sources

| Region | Model Type(s) Anomaly | | No of points | Max (mGal) | Min (mGal) | Mean (mGal) | Std. dev (mGal) | Source |
|---|---|---|---|---|---|---|---|---|
| Akure | Gravity | EGM2008 | 59 | 50.536 | 43.111 | 47.873 | 2.035 | ICGEM (2023) |
| | | SGG-UGM | 59 | 16.526 | 15.531 | 16.118 | 0.274 | |
| | | XGM2019e | 59 | 16.532 | 15.537 | 16.124 | 0.274 | |
| | Height | EGM2008 | 59 | 25.208 | 24.749 | 25.028 | 0.121 | |
| | | SGG-UGM | 59 | 23.868 | 23.654 | 23.779 | 0.057 | |
| | | XGM2019e | 59 | 23.875 | 23.661 | 23.787 | 0.057 | |

Table 6 outlines GGM-derived gravity anomaly datasets for Gombe, showing significant variations across models, with EGM2008 yielding a maximum gravity anomaly of 1.141 mGal, while SGG-UGM and XGM2019e display both positive and negative anomalies, sourced from ICGEM (2023).

**Table 6.** Summary of GGM-Gravity Anomaly and sources

| Region | Model Type(s) Anomaly | | No of points | Max (mgal) | Min (mgal) | Mean (mgal) | Std. dev (mgal) | Source |
|---|---|---|---|---|---|---|---|---|
| Gombe | Gravity | EGM2008 | 330 | 1.141 | 0.396 | 0.929 | 0.158 | ICGEM (2023) |
| | | SGGUGM | 330 | 1.350 | -1.482 | 0.194 | 0.647 | |
| | | XGM2019e | 330 | 0.945 | -0.093 | 0.445 | 0.237 | |
| | Height | EGM2008 | 330 | 17.326 | 17.286 | 17.313 | 0.009 | |
| | | SGGUGM | 330 | 17.349 | 17.299 | 17.332 | 0.011 | |
| | | XGM2019e | 330 | 17.362 | 17.319 | 17.347 | 0.009 | |

Table 7 summarizes the DEM-based elevation datasets for Akure and Gombe, with Akure's elevation ranging from 284 m to 408.976 m, while Gombe has higher variations with elevations reaching up to 448.746 m, sourced from USGS (2023).

**Table 7.** Summary of Digital Elevation Models (DEM) and sources

| Region | Elevation Model Type(s) | No of points | Max. (m) | Min (m) | Mean (m) | Std. dev (m) | Source |
|---|---|---|---|---|---|---|---|
| Akure | ALSO PALSAR | 59 | 350.086 | 288.825 | 334.393 | 10.562 | ICGEM (2023) |
| | ASTER | 59 | 350.000 | 284.000 | 330.610 | 11.721 | |
| | TANDEM | 59 | 408.976 | 341.133 | 379.343 | 15.413 | |
| Gombe | ALOS PALSAR | 330 | 448.746 | 291 | 361.329 | 44.161 | |
| | ASTER | 330 | 428.899 | 271.972 | 341.562 | 44.040 | |
| | TANDEM | 330 | 445.741 | 289.320 | 358.520 | 44.281 | |

Table 8 presents the validation datasets for Akure and Gombe, including GPS/leveling, gravimetric geoid heights, and orthometric heights, with Akure's geoid heights averaging 13.295 m and Gombe's orthometric heights reaching a maximum of 440.299 m. These data were sourced from Tata *et al.* (2019); Idowu (2006), and SNEPCO (1995).

**Table 8.** Summary of validation dataset and sources obtained within Akure and Gombe area

| Study area | Parameters | No of points | Mean (m) | Max. (m) | Min (m) | Std. dev (m) | Source |
|---|---|---|---|---|---|---|---|
| Akure | GPS/Levelling | 59 | 13.389 | 14.820 | 11.549 | 0.672 | Tata *et al.* (2019) |
| | Gravimetric | 59 | 13.295 | 14.551 | 11.201 | 0.617 | |
| | Ellipso. Heights | 59 | 347.748 | 363.926 | 301.375 | 10.959 | |
| | Ortho. Heights | 59 | 334.393 | 350.086 | 288.825 | 10.562 | |
| Gombe | Ortho. Heights | 330 | 353.804 | 440.299 | 284.502 | 44.152 | SNEPCO (1995) |

*Data Processing*

A three-phase computational process was adopted for the study. Phase one (1) involves preliminary processing, which consists of steps 1 to 5, while phase (2) involves the fitting of different spatial SLSC and NSLSC covariance models, which consists of steps 6 and 7. And lastly, phase 3 consists of steps eight and step 9. Each phase involves the process of evaluating all the different mathematical formulations represented by Equations 13 to 23. These were needed for the local gravimetric geoid estimation using the LSC technique (Schwarz and LaChapelle, 1980; Tscherning, 1994; Saadon *et al.*, 2021).

**Phase One (Preliminary Processing):**

STEP 01: Computation of Station Gravity Reductions (Free-air and Bouguer):

$$\boldsymbol{g_{FA_i}} = \boldsymbol{g_{obs}} + \boldsymbol{\delta g_F} = \boldsymbol{g_{obs}} - 0.3086h \quad (13)$$

$$g_{B_i} = g_{obs} + \delta g_B = g_{obs} + 2\pi K\rho h \quad (14)$$

STEP 02: Computation of Station Normal Gravity:

$$\boldsymbol{\gamma_{obs}} = \boldsymbol{\gamma_o}\,(1 + 0.0052790414\,\mathrm{Sin}2\phi + 0.0000232718\,\mathrm{Sin}4\phi) \quad (15)$$

STEP 03: Computation of Station Gravity Anomalies:

$$\Delta \boldsymbol{g_{FA}}(\boldsymbol{P_i}) = \boldsymbol{g_{FA_i}} - \boldsymbol{\gamma_{obs}} \quad (16)$$

$$\Delta g_B(P_i) = g_{B_i} - \boldsymbol{\gamma_{obs}} \quad (17)$$

STEP 04: Computation of Terrain Effect:

$$\boldsymbol{\xi_{RTM}}(\boldsymbol{P_i}) = \frac{\Delta \boldsymbol{g_B}(\boldsymbol{P_i})}{\bar{\gamma}}\boldsymbol{H^2} \quad (18)$$

**Phase Two (Fitting Spatially-varying model):**

STEP 05: Remove Phase (The effect of the Global Earth Gravity field model):

$$\Delta \boldsymbol{g_{res}}(\boldsymbol{P_i}) = \Delta \boldsymbol{g_{FA}}(\boldsymbol{P_i}) - \Delta \boldsymbol{g_{GGM}}(\boldsymbol{P_i}) \quad (19)$$

STEP 06: Fitting Spatially-varying model (SLSC **and** NSLSC) residual to gravity field:

$$\mathrm{S}\boldsymbol{T_{res}}(\boldsymbol{P_i}) = \mathrm{S}\boldsymbol{C}_{\boldsymbol{T_{res}}\Delta \boldsymbol{g_{res}}(\boldsymbol{P_{ij}})} * \mathrm{S}\boldsymbol{C}^{-1}_{\Delta \boldsymbol{g_{res}}\Delta \boldsymbol{g_{res}}(\boldsymbol{P_{ij}})} * \Delta \boldsymbol{g_{res}}(\boldsymbol{P_i})$$

$$\boldsymbol{NsT_{res}}(\boldsymbol{P_i}) = \mathrm{NS}\boldsymbol{C}_{\boldsymbol{T_{res}}\Delta \boldsymbol{g_{res}}(\boldsymbol{P_{ij}})} * \boldsymbol{N}\mathrm{S}\boldsymbol{C}^{-1}_{\Delta \boldsymbol{g_{res}}\Delta \boldsymbol{g_{res}}(\boldsymbol{P_{ij}})} * \Delta \boldsymbol{g_{res}}(\boldsymbol{P_i}) \quad (20)$$

STEP 07: Residual height anomalies (SLSC **and** NSLSC - quasi-geoid surface):

$$\mathrm{s}\boldsymbol{\xi_{res}}(\boldsymbol{P_i}) = \frac{\boldsymbol{sT_{res}}(\boldsymbol{P_i})}{\boldsymbol{\gamma}(\boldsymbol{P_i})}$$

$$\mathrm{Ns}\boldsymbol{\xi_{res}}(\boldsymbol{P_i}) = \frac{\boldsymbol{NsT_{res}}(\boldsymbol{P_i})}{\boldsymbol{\gamma}(\boldsymbol{P_i})}. \quad (21)$$

**Phase Three (Final geoid compilation):**

STEP 08 Restore Phase SLSC **and** NSLSC -Complete Quasi-Geoid Height Anomalies:

$$\mathrm{S}\boldsymbol{\xi}(\boldsymbol{P_i}) = \boldsymbol{\xi GGM}(\boldsymbol{P_i}) + \boldsymbol{\xi RTM}(\boldsymbol{P_i}) + \mathrm{S}\boldsymbol{\xi_{res}}(\boldsymbol{P_i})$$

$$\mathrm{NS}\boldsymbol{\xi}(\boldsymbol{P_i}) = \boldsymbol{\xi GGM}(\boldsymbol{P_i}) + \boldsymbol{\xi RTM}(\boldsymbol{P_i}) + \mathrm{NS}\boldsymbol{\xi_{res}}(\boldsymbol{P_i}) \quad (22)$$

STEP 09: SLSC **and** NSLSC Geoid Heights Based on Molodensky algorithm:

$$\begin{aligned} \mathrm{SN}(\boldsymbol{P_i}) &= \mathrm{S}\boldsymbol{\xi}(\boldsymbol{P_i}) + \frac{\Delta_{g_B}}{\bar{\gamma}}\boldsymbol{H}(\boldsymbol{P_i}) \\ \mathrm{NSN}(\boldsymbol{P_i}) &= \mathrm{NS}\boldsymbol{\xi}(\boldsymbol{P_i}) + \frac{\Delta_{g_B}}{\bar{\gamma}}\boldsymbol{H}(\boldsymbol{P_i}) \end{aligned} \tag{23}$$

*Research Hypothesis*

Two hypotheses were formulated for this study:

**1). Null Hypothesis ($\boldsymbol{H_{0_1}}$):** There are no significant differences in the mean computed between the results obtained from SLSC and NSLSC techniques in the estimated local gravimetric geoid. These are mathematically expressed as:

$$\mathbf{H_{0_1}}: \mu^{\mathrm{SLSC}} = \mu^{\mathrm{NSLSC}} \tag{24a}$$

**Alternative Hypothesis ($\boldsymbol{H_{A_1}}$):** There is. These are mathematically expressed as:

$$\mathbf{H_{A_1}}: \mu^{\mathrm{SLSC}} \neq \mu^{\mathrm{NSLSC}} \tag{24b}$$

where: SLSC = Stationary and NSLSC = Nonstationary covariance approaches.

**2). Null Hypothesis ($\mathbf{H_{0_2}}$):** There is no significant difference between the Mean of computed Best-fit (Optimum) values obtained from hypothesis test (1) above and those obtained from existing Gravimetric, GPS/Leveling geoidal undulations or Orthometric heights of the stations. These are mathematically expressed as:

$$\mathbf{H_{0_{2_i}}}: \mu^{\mathrm{BEST-fit}} = \mu^{\mathrm{Existing}}_{\mathrm{Gravimetric}} \tag{25a}$$

$$\mathbf{H_{0_{2_j}}}: \mu^{\mathrm{BEST-fit}} = \mu^{\mathrm{Existing}}_{\mathrm{GPS/Leveling}} \tag{26a}$$

$$\mathbf{H_{0_{2_k}}}: \mu^{\mathrm{BEST-fit}} = \mu^{\mathrm{Existing}}_{\mathrm{Orthometrics}} \tag{27a}$$

**Alternative Hypothesis ($\mathbf{H_{A_4}}$):** There is. These are mathematically expressed as:

$$\mathbf{H_{A_{2_i}}}: \mu^{\mathrm{Computed}} \neq \mu^{\mathrm{Existing}}_{\mathrm{Gravimetric}} \tag{25b}$$

$$\mathbf{H_{A_{2_j}}}: \mu^{\mathrm{Computed}} \neq \mu^{\mathrm{Existing}}_{\mathrm{GPS/Leveling}} \tag{26b}$$

$$\mathbf{H_{A_{2_k}}}: \mu^{\mathrm{Computed}} \neq \mu^{\mathrm{Existing}}_{\mathrm{Orthometric\ Heights}} \tag{27b}$$

*Statistical analysis*

Statistical hypotheses test One (1) was implemented using the SPSS (23) version's sub-routine, predefined for MANOVA via the General Linear Model (GLM) at both 95% and 99.9% confidence intervals for SLSC and NSLSC, respectively. For hypothesis two (2), the study implemented the Paired Samples Statistics, Correlation, and T-Test to compare the means of two or more related groups and determine if a significant difference existed between the paired observations. This analysis was also conducted at 95% and 99.9% confidence intervals.

## Results

In this study, the datasets obtained were employed within the mathematical formulations previously outlined summarily in steps 1 to 9 of equations 13 to 23.

Table 9 presents the results from Phase Two and Three processing obtained from the most suitable model (Matern, SGG-UM-GGM, and ALOS-DEM) within Akure, showing residual gravity field values, height anomalies, quasi-geoid heights, geoidal heights, and orthometric heights.

**Table 9.** Phases 2 and 3 sample results obtained within the Akure study area

| Station | X | Y | Phase Two | | Phase Three | | Ortho. Height (m) |
|---|---|---|---|---|---|---|---|
| | | | Residual field (m) | Residual height anomaly (m) | Quasi Height anomaly (m) | Geoidal Height (m) | |
| | (m) | (m) | Eqn. 20 | Eqn. 21 | Eqn. 22 | Eqn. 23 | |
| GPSA72S | 739272.08 | 804184.37 | -99.1538 | -0.0001 | 13.70014 | 13.67084 | 332.7992 |
| GPSA73S | 739057.83 | 804174.63 | -99.1526 | -0.0001 | 13.77826 | 13.74907 | 331.3974 |
| GPSA75S | 738721.93 | 804299.37 | -99.1913 | -0.0001 | 14.16897 | 14.14035 | 324.2477 |
| GPSA76S | 738465.8 | 804373.82 | -99.2146 | -0.0001 | 14.2675 | 14.23902 | 322.427 |
| GPSA77S | 738143.72 | 804499.99 | -99.2529 | -0.0001 | 14.38198 | 14.35366 | 320.2973 |

Meanwhile, Table 10 presents the sample results from Phase Two and Three analyses using the most suitable model (Exponential, EGM2008-GGM and TANDEM-DEM) within Gombe, showing residual gravity field values, height anomalies, quasi-geoid heights, geoidal heights, and orthometric heights.

**Table 10.** Phases 2 and 3 sample results obtained within Gombe study area

| Station | X | Y | Phase Two | | Phase Three | | Ortho. Height (m) |
|---|---|---|---|---|---|---|---|
| | | | Residual field (m) | Residual height anomaly (m) | Quasi Height anomaly (m) | Geoidal Height (m) | |
| | (m) | (m) | Eqn. 20 | Eqn. 21 | Eqn. 22 | Eqn. 23 | |
| V146840 | 673306 | 1222185 | -193.322 | -0.00019760 | 20.249 | 20.168 | 383.233 |
| V146860 | 673805 | 1222220 | -192.7841 | -0.00019705 | 20.237 | 20.156 | 377.744 |
| V146880 | 674303 | 1222268 | -192.269 | -0.00019652 | 20.225 | 20.145 | 373.155 |
| V146920 | 675273 | 1222421 | -191.357 | -0.00019559 | 20.199 | 20.120 | 372.480 |
| V146940 | 675738 | 1222262 | -190.820 | -0.00019504 | 20.188 | 20.110 | 364.090 |

Table 11 provides summary statistics for station geoidal undulation and processing time obtained within the Akure study area, comparing the SLSC and NSLSC techniques at 95% and 99.9% confidence intervals.

**Table 11.** Summary statistics obtained at 95% and 99.9% (C.I.) within the Akure study area

| Dependent Variable | LSC Techniques | 95% | 99.9% | 95% | 99.9% | 95% C.I. | | 99.9% C.I. | |
|---|---|---|---|---|---|---|---|---|---|
| | | Mean | | Std. Error | | Lower Bound | Upper Bound | Lower Bound | Upper Bound |
| Geoidal Undulation | SLSC | 14.273[a] | 14.273[a] | 0.025 | 0.025 | 14.224 | 14.323 | 14.190 | 14.356 |
| | NSLSC | 14.294[a] | 14.294[a] | 0.025 | 0.025 | 14.244 | 14.343 | 14.211 | 14.376 |
| Processing Time (Seconds) | SLSC | 8.210[a] | 8.210[a] | 0.000 | 0.000 | 8.210 | 8.210 | 8.210 | 8.210 |
| | NSLSC | 38.669[a] | 38.669[a] | 0.000 | 0.000 | 38.669 | 38.669 | 38.669 | 38.669 |

*Covariates appearing in the model are evaluated at the following values: Computed Orthometric Height = 320.10962377809270

Similarly, Table 12 presents summary statistics for station geoidal undulation and processing time obtained within the Gombe study area, comparing the SLSC and NSLSC techniques at 95% and 99.9% confidence intervals.

**Table 12.** Summary statistics obtained at 95% and 99.9% (C.I.) within the Gombe study area

| Dependent Variable | LSC Techniques | 95% | 99.9% | 95% | 99.9% | 95% C.I. | | 99.9% C.I. | |
|---|---|---|---|---|---|---|---|---|---|
| | | Mean | | Std. Error | | Lower Bound | Upper Bound | Lower Bound | Upper Bound |
| Geoidal Undulation | SLSC | 19.951[a] | 19.951[a] | 0.003 | 0.003 | 19.945 | 19.957 | 19.941 | 19.961 |
| | NSLSC | 19.900[a] | 19.900[a] | 0.003 | 0.003 | 19.895 | 19.906 | 19.891 | 19.910 |
| Processing Time (Seconds) | SLSC | 91.505[a] | 91.505[a] | 0.000 | 0.000 | 91.505 | 91.505 | 91.505 | 91.505 |
| | NSLSC | 373.663[a] | 373.663[a] | 0.000 | 0.000 | 373.663 | 373.663 | 373.663 | 373.663 |

*Covariates appearing in the model are evaluated at the following values: Computed Orthometric Height = 319.28446159531140.

Figure 2 visually compares geoidal undulation and processing time for SLSC and NSLSC techniques within Akure at 95% and 99.9% confidence intervals.

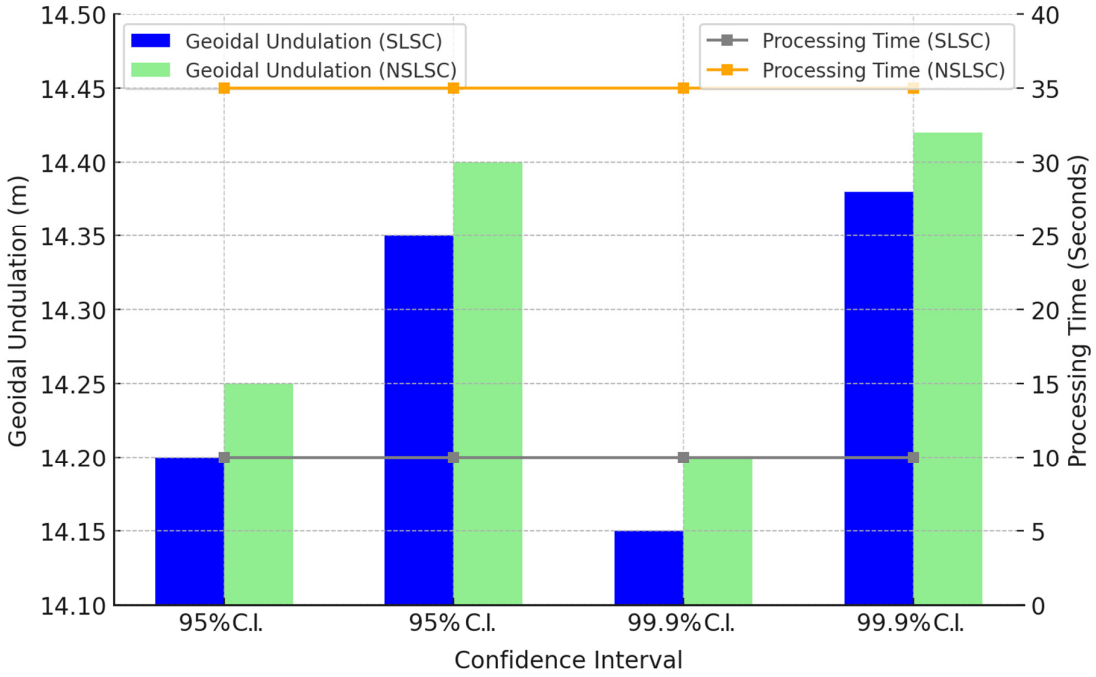


**Figure 2.** Geoidal undulation and processing time comparison using SLSC and NSLSC in Akure

Figure 3 is a geoidal undulation contour map representing variations in geoidal height across a specific region, with undulation values ranging from approximately 9.8 m to 14.2 m, depicted through color gradients and contour lines based on easting and northing coordinates

Figure 4 presents a comparison of geoidal undulation and processing time using SLSC and NSLSC techniques in Gombe at 95% and 99.9% confidence intervals, showing that NSLSC results in higher undulation values and significantly longer processing times compared to SLSC.

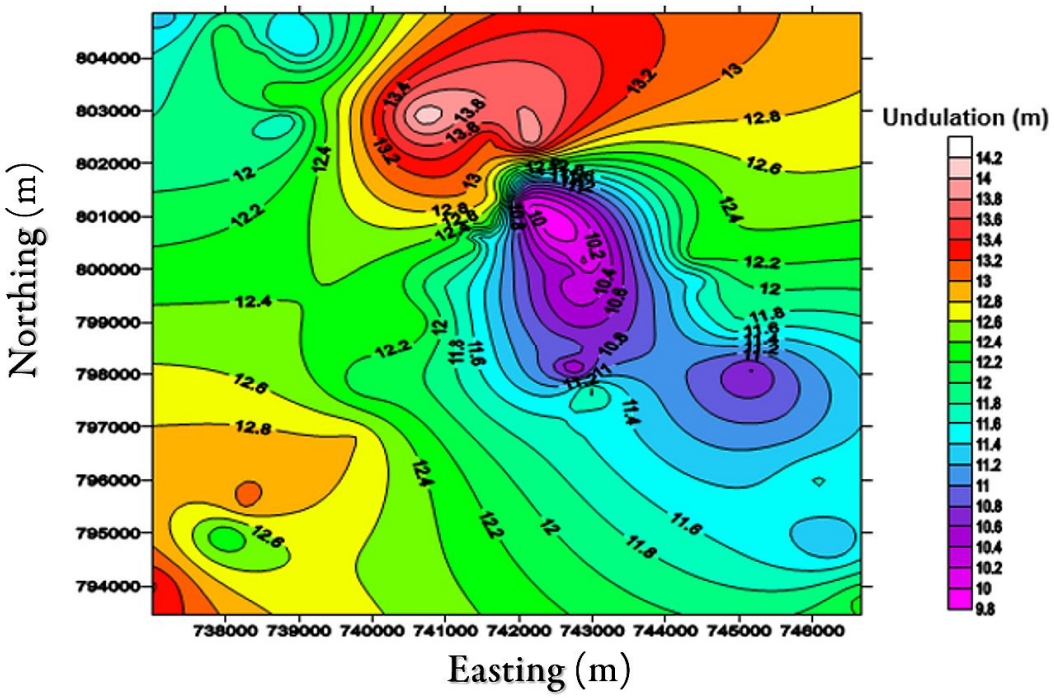


**Figure 3.** Geoidal undulation contour plot within the Akure study area

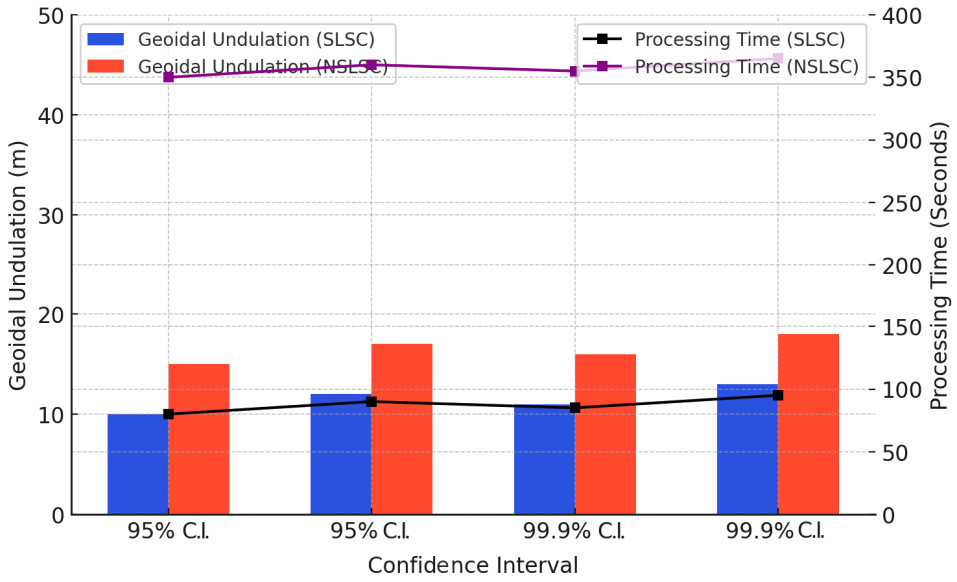


**Figure 4.** Geoidal undulation and processing time comparison using SLSC and NSLSC in Gombe

Figure 5 presents a contour plot of the best-fit SLSC computed orthometric height within the Gombe study area. The color gradient represents variations in orthometric height, with higher elevations indicated by warm colors (red and orange) and lower elevations by cool colors (blue and purple). The contour lines illustrate the topographic variation, providing insight into the terrain undulation and elevation distribution within the region.

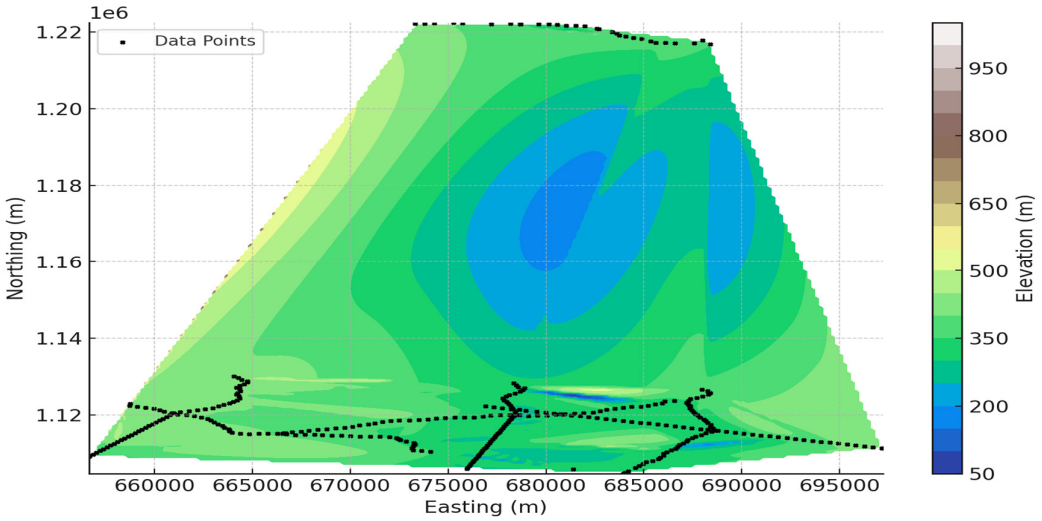


**Figure 5.** Contour plot of orthometric heights within the Gombe study area

### Statistical Test Results

For the statistical hypothesis testing one (1), the SPSS (23) version's sub-routine, predefined for MANOVA via the General Linear Model (GLM), was activated. Here, pairwise comparison results for SLSC and NSLSC outputted from the package are summarized and presented for the Akure and Gombe study areas in Tables 13 and 14.

**Table 13.** Pairwise comparison for Hypothesis testing one (1) within Akure study area

| Dependent Variable | (I) LSC Techniques | (J) LSC Techniques | Mean Difference (I-J) | Std. Error | Sig.[b] | 95% C. I for Difference[b] | | 99.9% C. I for Difference[b] | |
|---|---|---|---|---|---|---|---|---|---|
| | | | | | | Lower Bound | Upper Bound | Lower Bound | Upper Bound |
| Geoidal Undulation | SLSC | NSLSC | -0.02 | 0.036 | 0.567 | -0.09 | 0.049 | -0.137 | 0.097 |
| | NSLSC | SLSC | 0.02 | 0.036 | 0.567 | -0.049 | 0.09 | -0.097 | 0.137 |
| Processing Time (Seconds) | SLSC | NSLSC | -30.459* | 0 | 0 | -30.46 | -30.46 | -30.46 | -30.46 |
| | NSLSC | SLSC- | 30.459* | 0 | 0 | 30.459 | 30.459 | 30.459 | 30.459 |

Based on Estimated Marginal Means: *. The mean difference is significant at the 0.05 level; *. The mean difference is significant at the .001 level.

b. Adjustment for multiple comparisons: Least Significant Difference (equivalent to no adjustments).

**Table 14.** Pairwise comparison for Hypothesis testing one (1) within Gombe study area

| Dependent Variable | (I) LSC Techniques | (J) LSC Techniques | Mean Difference (I-J) | Std. Error | Sig.[b] | 95% C.I for Difference[b] | | 99.9% C. I for Difference[b] | |
|---|---|---|---|---|---|---|---|---|---|
| | | | | | | Lower Bound | Upper Bound | Lower Bound | Upper Bound |
| Geoidal Undulation | SLSC | NSLSC | 0.051* | 0.004 | 0 | 0.043 | 0.059 | 0.037 | 0.065 |
| | NSLSC | SLSC | -0.051* | 0.004 | 0 | -0.059 | -0.043 | -0.065 | -0.037 |
| Processing Time (Seconds) | SLSC | NSLSC | -282.158 | 0 | . | -282.16 | -282.16 | -282.16 | -282.16 |
| | NSLSC | SLSC | 282.158 | 0 | . | 282.158 | 282.158 | 282.158 | 282.158 |

Based on Estimated Marginal Means: *. The mean difference is significant at the 0.05 level; *. The mean difference is significant at the .001 level.

b. Adjustment for multiple comparisons: Least Significant Difference (equivalent to no adjustments).

Table 15 presents the paired samples correlation results for hypothesis testing within the Akure study area, showing negative correlations between the best-fit model and existing GRAV (r = -0.27, p = 0.000) and GPS/Level models (r = -0.303, p = 0.000), while a perfect correlation (r = 1, p = 0.000) is observed between computed and existing orthometric heights.

**Table 15.** Paired sample correlation results obtained between computed and existing models within the Akure study area

| Content | | Mean | N | Std. Deviation | Std. Error Mean | Correlation | Sig. |
|---|---|---|---|---|---|---|---|
| Pair 1 | Best-Fit Model | 14.28343 | 3186 | 1.177921 | 0.020869 | -0.27 | 0 |
| | Existing (GRAV) | 13.29519 | 3186 | 0.612273 | 0.010847 | | |
| Pair 2 | Best-Fit Model | 14.28343 | 3186 | 1.177921 | 0.020869 | -0.303 | 0 |
| | Existing (GPS/LEVEL) | 13.3885 | 3186 | 0.665866 | 0.011797 | | |
| Pair 3 | Computed Height | 320.1096 | 3186 | 11.03857 | 0.195564 | 1 | 0 |
| | Existing Height | 334.393 | 3186 | 10.47366 | 0.185556 | | |

Table 16 presents the paired samples test results for the Akure study area, indicating statistically significant differences (p = 0.000) between the best-fit model and existing GRAV and GPS/Level models, as well as between computed and existing orthometric heights, with 95% confidence intervals ranging from (0.93728 to 1.03920), (0.84218 to 0.94769), and (-14.3051 to -14.2617) m, and 99.9% confidence intervals from (0.90264 to 1.07385), (0.80631 to 0.98355), and (-14.31987 to -14.2469) m, respectively.

**Table 16.** Paired samples test results obtained between computed and existing models within the Akure study area

| Pair | Model | Paired Differences | | | | | | | t | df | Sig. (2-tailed) |
|---|---|---|---|---|---|---|---|---|---|---|---|
| | | Mean | Std. Dev. | Std. Error Mean | 95% C. I of the Difference | | 99.9% C. I of the Difference | | | | |
| | | | | | Lower | Upper | Lower | Upper | | | |
| 1 | Best-ft Model) vs. Existing Model (GRAV) | 0.988242 | 1.467091 | 0.025992 | 0.93728 | 1.039204 | 0.9026367 | 1.0738482 | 38.022 | 3185 | 0 |
| 2 | Best-ft Model) vs. Existing Model (GPS/LEVEL) | 0.894931 | 1.518723 | 0.026906 | 0.842175 | 0.947686 | 0.806312 | 0.9835491 | 33.261 | 3185 | 0 |
| 3 | Computed Orthometric Height vs. Exist Orthometric Height | -14.28339 | 0.625249 | 0.01108 | -14.3051 | -14.26166 | -14.31987 | -14.2469 | -1289.455 | 3185 | 0 |

Table 17 presents the paired samples correlation results for hypothesis testing within the Gombe study area, showing a strong positive correlation (r = 0.982, p = 0.000) between computed and existing heights, while a moderate positive correlation (r = 0.534, p = 0.000) is observed between the geoidal undulation model and computed height.

**Table 17.** Paired sample correlation results obtained between computed and existing models within the Gombe study area

| Pair/Computed and existing models | | Mean | N | Std. Deviation | Std. Error Mean | Correlation | Sig. |
|---|---|---|---|---|---|---|---|
| Pair 1 | Computed Height | 319.284462 | 17820 | 45.616823 | 0.341721 | 0.982 | 0.000 |
| | Existing Height | 353.803714 | 17820 | 44.086712 | 0.330258 | | |
| Pair 2 | Geoidal Undulation Model | 19.925695 | 17820 | 0.340805 | 0.002553 | 0.534 | 0.000 |
| | Computed Height | 319.284462 | 17820 | 45.616823 | 0.341721 | | |

Table 18 presents the paired samples test results for the Gombe study area, showing significant differences (p = 0.000) between computed and existing orthometric heights, as well as between best-fit geoidal undulation and computed orthometric height, with 95% confidence intervals ranging from (-34.6468 to -34.3917) m and (-300.026 to -298.6916) m, and 99.9% confidence intervals from (-34.7333 to -34.3052) m and (-300.4789 to -298.2386) m, respectively.

**Table 18.** Paired samples test results obtained between computed and existing models within the Gombe study area

| Pair | Model | Paired Differences | | | | | | | t | df | Sig. (2-tailed) |
|---|---|---|---|---|---|---|---|---|---|---|---|
| | | Mean | Std. Dev. | Std. Error Mean | 95% C. I of the Difference | | 99.9% C. I of the Difference | | | | |
| | | | | | Lower | Upper | Lower | Upper | | | |
| 1 | Computed Orthometric Height vs. Exist Orthometric Height | -34.519252 | 8.6839538 | 0.065053 | -34.64668 | -34.391743 | -34.733344 | -34.30516 | -530.637 | 17819 | 0 |
| 2 | Best-fit Geoidal undulation vs. Computed Orthometric Height | -299.3587664 | 45.4358144 | 0.340365 | -300.026 | -298.69162 | -300.47893 | -298.2386 | -879.524 | 17819 | 0 |

Figure 6 presents the estimated marginal means of geoidal undulation in the Akure study area using the SGG-UM-2-GGM model, comparing different covariance models (Gaussian, Exponential, and Matérn) for SLSC and NSLSC techniques.

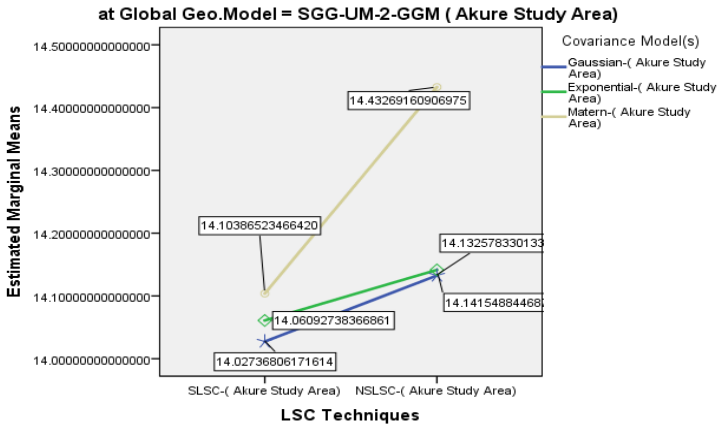


**Figure 6.** The estimated marginal means of geoidal undulation for the Akure study area across three covariance models: Gaussian, Exponential, and Matérn based on SGG-UM-GGM

Figure 7 presents the estimated marginal means of processing time (in seconds) for different covariance models (Gaussian, Exponential, and Matérn) in the Akure study area, evaluated at a computed orthometric height of 319.2845 m.

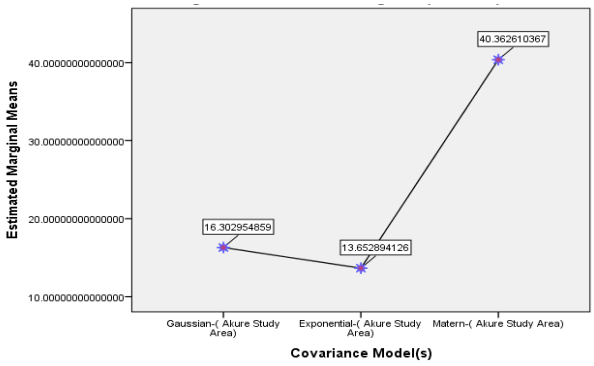


**Figure 7.** Processing time of the three covariance models within Akure

Figure 8 illustrates the estimated marginal means of geoidal undulation for the Gombe study area using the EGM2008 global geopotential model. The plot compares different covariance models (Gaussian, Exponential, and Matérn) across two Least Squares Collocation (LSC) techniques: Stationary LSC (SLSC) and Non-Stationary LSC (NSLSC).

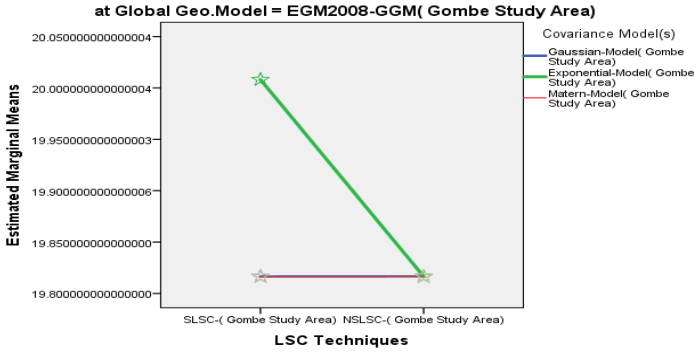


**Figure 8.** The estimated marginal mean values of geoidal undulation for the Akure study area across three covariance models: Gaussian, Exponential, and Matérn based on EGM2008-GGM

Figure 9 presents the estimated marginal means of processing time (in seconds) for different covariance models (Gaussian, Exponential, and Matérn) in the Gombe study area, evaluated at a computed orthometric height of 319.2845 m.

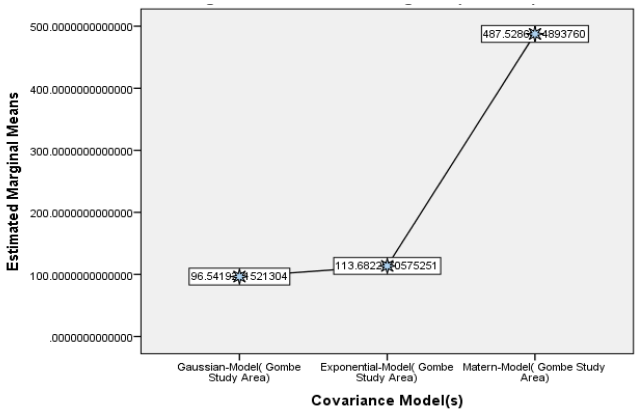


**Figure 9.** Processing time of the three covariance models within Gombe

## Discussion

*Comparison of Geoidal Undulation Estimates and Processing Time within Akure Using SLSC and NSLSC Techniques*

From Table 13, it can be observed that the geoidal undulation for the Akure study area using the Stationary Least Squares Collocation (SLSC) technique had a mean of 14.273 m (SE = 0.025 m) with a 95% confidence interval of [14.224 m, 14.323 m], while the Non-Stationary Least Squares Collocation (NSLSC) technique produced a slightly higher mean of 14.294 m (SE = 0.025 m) with a 95% confidence interval of [14.244 m, 14.343 m]. The processing time for the SLSC was significantly shorter at 8.210 seconds (SE = 0.000), compared to the NSLSC, which required 38.669 seconds (SE = 0.000). The 99.9% confidence intervals for geoidal undulation were [14.190 m, 14.356 m] for SLSC and [14.211 m, 14.376 m] for NS-SLSC. All estimates were calculated with the covariate of computed orthometric height evaluated at 320.11 m.

The NSLSC technique takes significantly longer, about 30.46 seconds, than the SLSC technique. The difference in processing times suggests that SLSC is a faster method, making it potentially more efficient for handling large datasets or applications requiring quick results. In contrast, NSLSC may be better suited for situations where accuracy is prioritized over speed, as its longer processing time may be attributed to more complex calculations within its algorithm. The covariate, Computed Orthometric Height, was held constant at 320.11m in both cases, indicating that processing time differences are likely due to the techniques themselves rather than variations in the covariate. Hence, while NSLSC provides more precise results, its significantly higher processing time may limit its practical use in situations demanding faster computations.

*Impact of Covariance Models on Geoidal Undulation and Processing Time within Akure*

A review of Figure 6 reveals a comparison of the Estimated Marginal Means of geoidal undulation for the Akure study area across three covariance models: Gaussian, Exponential, and Matérn based on the SGG-UM-GGM as the best-fit GGM dataset. The Gaussian and Exponential models show very similar results, with values of 14.2733 m and 14.2732 m, respectively, while the Matérn model yields a higher value of 14.3037 m. This suggests that the Matérn model may better account for spatial variability or provide a more refined estimation of the geoidal undulation within Akure. These differences highlight the importance of selecting an appropriate covariance model to improve the accuracy of geodetic computations.

Figure 7 displays the Estimated Marginal Means of Processing Time (Seconds) for these three different covariance models. The Gaussian model shows an estimated processing time of approximately 16.30 seconds, the Exponential model has a processing time of about 13.65 seconds, and the Matérn model has the highest processing time at 40.36 seconds. This indicates that the Matérn covariance model requires significantly more time compared to the Gaussian and Exponential models, with a difference of 23.06 seconds compared to the Exponential and 24.06 seconds compared to the Gaussian. The difference in processing times suggests that the Exponential and Gaussian models are more computationally efficient, while the Matérn model could be more complex, requiring more time to process. This reflects the intricacy of the model's calculations, where Matérn provides a more detailed fit but at the cost of increased processing time.

The covariate, Computed Orthometric Height, was constant at 320.11 m for all models, meaning that the observed differences in processing times are likely due to the chosen covariance model rather than the covariate itself. If speed is a priority, the Exponential and Gaussian models are preferable, but for potentially more accurate or detailed analysis, the Matérn model could be considered despite the longer processing time.

*Comparison of Geoidal Undulation Estimates and Processing Time within Gombe Using SLSC and NSLSC Techniques*

For the Gombe study area, Table 8 reveals the geoidal undulation estimated using the Stationary Least Squares Collocation (SLSC) technique. This had a mean of 19.951 m (SE = 0.003 m), with a 95% confidence interval of [19.945 m, 19.957 m], while the Non-Stationary Least Squares Collocation (NSLSC) technique produced a slightly lower mean of 19.900 m (SE = 0.003 m), with a 95% confidence interval of [19.895 m, 19.906m]. The processing time for the SLSC was 91.505 seconds (SE = 0.000), which was considerably shorter than the 373.663 seconds (SE = 0.000) required for the NSLSC. The 99.9% confidence intervals for geoidal undulation were [19.941 m, 19.961 m] for SLSC and [19.891 m, 19.910 m] for NS-SLSC. These estimates were computed with the covariate of orthometric height evaluated at 319.28 m.

The SLSC technique provides a higher geoidal undulation estimate of 19.951 m, while the NSLSC technique shows a lower value of 19.900 m. This significant difference suggests that the SLSC approach is more sensitive in capturing the local variations in the geoid for the Gombe study area. The results indicate that the choice of the LSC technique has a notable impact on geoidal undulation values in this region.

*Impact of Covariance Models on Geoidal Undulation and Processing Time within Gombe*

Figure 8 illustrates the Estimated Marginal Means of Geoidal Undulation for the Gombe study area, evaluated using three covariance models: Gaussian, Exponential, and Matérn, at a computed orthometric height of 319.285 m. The Exponential model yielded the highest geoidal undulation value of 19.976 m, indicating a stronger fit to local geoid variations. Conversely, the Gaussian and Matérn models produced similar and lower values of 19.900 m, suggesting a relatively smoother representation of local geoid undulations. Figure 9 further compares the processing times for the three covariance models in the Gombe study area. The Gaussian model has a processing time of approximately 96.54 seconds, the Exponential model shows 113.68 seconds, and the Matérn model has a significantly higher processing time of about 487.53 seconds. The sharp increase in processing time for the Matérn model suggests it is the most computationally intensive of the three.

**Hypothesis Testing**

*Paired Samples Analysis of Geoidal Undulation and Orthometric Heights*

Table 16 reveals the paired samples test within the Akure study area and evaluates the statistical differences between the best-fit model and existing models (GRAV and GPS/LEVEL) and between computed and existing orthometric heights. The results show mean differences of 0.988242 and 0.894931 for the best-fit model versus GRAV and GPS/Level models, respectively, with both comparisons having low standard errors (0.025992 and 0.026906) and confidence intervals indicating significant positive differences. The computed orthometric heights differ significantly from the existing orthometric heights by -14.28339, with a small

standard error (0.01108) and tight-bound confidence intervals. The extremely high t-values (38.022, 33.261, and -1289.455) and a significance value of 0 ($p < 0.05$) for all comparisons confirm that these differences are statistically significant, indicating a strong deviation between the computed and reference models. As shown in Table 18, the paired samples test within the Gombe study area reveals significant differences in orthometric height estimations. The comparison between computed and existing orthometric heights reveals a mean difference of 34.52 meters, with a standard deviation of 8.68 meters. The 95% confidence interval ranges from 34.39 to 34.65 meters, while the 99.9% confidence interval extends from 34.31 to 34.73 meters. The large t-value (530.64) with 17,819 degrees of freedom and a significance level of 0 indicates a statistically significant difference. Similarly, the comparison between the best-fit geoidal undulation and computed orthometric heights shows an even greater mean difference of 299.36 meters, with a standard deviation of 45.44 meters. The 95% confidence interval spans from 298.69 to 300.03 meters, while the 99.9% confidence interval ranges from 298.24 to 300.48 meters. A t-value of 879.52, with the same degrees of freedom and a significance level of 0, further confirms the statistical significance of this difference. These results highlight substantial discrepancies in orthometric height estimations, underscoring the need for further investigation into potential errors or biases in the geoid modeling process for the Gombe study area.

## Conclusions

This research investigates the computation of a local gravimetric geoid using Stationary and Nonstationary Least Squares Collocation (SLSC and NSLSC) techniques across two distinct terrains in Nigeria: Akure South Local Government Area in Ondo State, representing mountainous terrain, and the Gombe-Kolmani Basin in Gombe State, characterized by gently rolling terrain. High-quality terrestrial gravity data, geopotential models, and digital elevation models (DEMs) were used to ensure reliable geoid estimation. The methodology involved applying three different SLSC and NSLSC covariance models, integrated with the Molodensky model algorithm, within the Remove-Compute-Restore (R-C-R) framework. Various global geopotential and digital terrain models were utilized to determine geoidal undulations. Statistical analyses, including Multivariate Analysis of Variance (MANOVA) and paired t-tests, were conducted to assess differences in geoid estimates and processing efficiency between the two LSC techniques.

The results indicate that in Akure, the mean difference in geoidal undulation estimates between SLSC and NSLSC was -0.020 meters, with a p-value of 0.567, showing no statistically significant difference. This implies that both techniques yield similar geoid heights in mountainous terrain. However, in Gombe, the mean difference was 0.051 meters, with a p-value of $< 0.001$, indicating a significant impact of the chosen LSC technique on geoid estimates in gently rolling terrain. Regarding computational efficiency, SLSC was significantly faster in both study areas. In Akure, it reduced processing time by 30.459 seconds, and in Gombe, by 282.158 seconds, both with p-values $< 0.001$. These findings highlight the computational advantage of SLSC over NSLSC.

Validation of the geoid model was conducted by comparing the best-fit model with existing gravimetric and GPS/leveling geoid models. In Akure, no significant difference was observed between the estimated geoidal undulations and GPS/leveling-derived geoid heights, confirming the accuracy of the model. In Gombe, however, discrepancies were observed, indicating the need for further refinement in this region. The study confirms that NSLSC provides higher precision in mountainous terrains, while SLSC is computationally more efficient, making it a preferable choice in gently rolling terrains. NSLSC demands extensive computational resources due to the inversion of large covariance matrices, particularly when using the Matérn model. On the other hand, SLSC, while faster, assumes stationarity in the covariance structure, which may not adequately capture spatial variations in complex terrains. Also, using the GGM dataset in Akure for both approaches, the standard deviations for both approaches yielded 1.538476 m and 1.538454 m respectively. Furthermore, using the DEM dataset in Akure for both approaches, the standard deviations for both approaches yielded 0.943200

m and 0.943198 m respectively. The results obtained from using the GGM datasets in Gombe yielded standard deviations of 0.340943 m and 0.338443 m for the SLSC and NSLSC techniques, respectively, while the DEM datasets used in Gombe produced standard deviations of 0.352285 m and 0.352496 m for the two techniques, respectively. While high-resolution DEMs and GGMs were used, sparse terrestrial gravity observations can introduce interpolation uncertainties, affecting model reliability. To improve geoid modeling, a hybrid approach combining SLSC and NSLSC to be known as adaptive covariance modeling is hereby proposed. The concept is hitched to the scenario where the covariance function can transit between stationary and nonstationary structures based on terrain complexity. This would enhance efficiency in homogeneous and non-homogeneous terrains while maintaining accuracy in regions with significant spatial variability. While the SLSC and NSLSC offer significant advancements in local geoid modeling, their computational and data limitations highlight the need for this hybrid approach; which is critical for engineering, surveying, and geophysical studies in topographically complex regions. For instance, in geodetic and engineering applications, pre-calculated height determination using GNSS leveling that will ensure reliable height conversions and reduce systematic errors in elevation data is feasible. This is particularly valuable in mountainous regions where standard models often struggle with high gravity field variability.

## Authors' Contributions

Conceptualization: A.A.T.; Investigation: A.A.T.; Methodology: A.A.T.; T.O.I. and H.T.; Resources: T.O.I. and H.T.; Software: A.A.T.; Supervision: T.O.I. and H.T.; Validation: T.O.I. and H.T.; Visualization: A.A.T.; Writing - original draft: A.A.T.

All authors read and approved the final manuscript.

## Acknowledgments

This research was not funded by any public, commercial, or non-profit organization. However, the corresponding author sincerely appreciates Dr. I. U. Nzelibe, Mr. Barnabas Jauro, Dr. Steven Tumba, Mr. Jackson Matapa, and Mr. Paul Oloyede, among others, for their time and, in some cases, financial support in obtaining data and materials for pre-analysis and validation, which contributed to the successful completion of this study.

## Conflict of Interests

The authors declare no conflicts of interest related to this article.

## References

Abd-Elmotaal HA (1998). An efficient technique for the computation of gravimetric quantities from geopotential Earth models. In: Forsberg R, Feissel M, Dietrich R (Eds). Geodesy on the Move. International Association of Geodesy Symposia Vol 119. Springer, Berlin, Heidelberg. *https://doi.org/10.1007/978-3-642-72245-5_25*

Al-Ajami H, Zaki A, Rabah M, El-Ashquer M (2022). A high-resolution gravimetric geoid model for Kuwait using the least-squares collocation. Frontiers in Earth Science 9:753269. *https://doi.org/10.3389/feart.2021.753269*

Alberts BA, Ditmar P, Klees R (2007). A new methodology to process airborne gravimetry data: advances and problems. In: Tregoning P, Rizos C (Eds). Dynamic Planet. International Association of Geodesy Symposia, Vol 130, 251-258. Springer, Berlin, Heidelberg. *https://doi.org/10.1007/978-3-540-49350-1_38*

Ayeni OO (1981). Statistical adjustment and analysis of data: (with applications in geodetic surveying and photogrammetry). Lagos: University of Lagos.

Barthelmes F (2018). Global Models. In: Grafarend E (Ed). Encyclopedia of Geodesy. Encyclopedia of Earth Sciences Series. Springer, Cham. *https://doi.org/10.1007/978-3-319-02370-0_43-2*

Collier P, Argeseanu V, Leahy F (1998). Distortion modeling and the transition to GDA94. Australian Surveyor 43(1):29-40. *https://doi.org/10.1080/00050347.1998.10558718*

Dagogo MJ, Francis F, Christian UE (2014). Fundamentals of Geodesy. Textbook. Published by Concept Publications Limited. 77, Shipeolu Street, Palm Grove, Lagos, Nigeria.

Darbeheshti N, Featherstone WE (2009). Non-stationary covariance function modeling in 2D least-squares collocation. Journal of Geodesy 83(6):495-508. *https://doi.org/10.1007/s00190-008-0267-0*

Darbeheshti N, Featherstone WE (2010). Tuning a gravimetric quasi geoid to GPS-levelling by non-stationary least-squares collocation. Journal of Geodesy 84(7):419-431. *https://doi.org/10.1007/s00190-010-0377-3*

Denker H, Torge W, Wenzel G, Ihde J, Schirmer U (2000). Investigation of different methods for the combination of gravity and GPS/levelling data. In: Schwarz KP (Ed). Geodesy Beyond 2000. International Association of Geodesy Symposia, Vol 121. Springer, Berlin, Heidelberg. *https://doi.org/10.1007/978-3-642-59742-8_23*

Duquenne H, Everaerts M, Lambot P (2005). Merging a gravimetric model of the geoid with GPS/Levelling data: An example in Belgium. In: Jekeli C, Bastos L, Fernandes J (Eds). Gravity, Geoid and Space Missions. International Association of Geodesy Symposia, Vol 129. Springer, Berlin, Heidelberg. *https://doi.org/10.1007/3-540-26932-0_23*

El-Ashquer M, Elsaka B, El-Fiky G (2017). EGY-HGM2016: an improved hybrid local geoid model for Egypt based on the combination of GOCE-based geopotential model with gravimetric and GNSS/leveling measurements. Arabian Journal of Geosciences 10:251. *https://doi.org/10.1007/s12517-017-3042-9 10 53115*

Ezeigbo CU (1988). Least squares collocation method for geoid and datum determination for Nigeria. PhD Thesis, Department of Surveying, University of Lagos, Nigeria.

Featherstone W (1998). Do we need a gravimetric geoid or a model of the Australian height datum to transform GPS heights in Australia? Australian Surveyor 43(4):273-280. *https://doi.org/10.1080/00050350.1998.10558758*

Forsberg R (1987). A new covariance model for inertial gravimetry and gradiometry. Journal of Geophysical Research: Solid Earth 92(B2):1305-1310. *https://doi.org/10.1029/jb092ib02p01305*

Goad CC, Tscherning CC, Chin MM (1984). Gravity empirical covariance values for the continental United States. Journal of Geophysical Research: Solid Earth 89(B9):7962-7968. *https://doi.org/10.1029/jb089ib09p07962*

Goli M, Foroughi I, Novák P (2019). Application of the one-step integration method for determination of the regional gravimetric geoid. Journal of Geodesy 93(9):1631-1644. *https://doi.org/10.1007/S00190-019-01272-8*

Guimarães GD, Blitzkow D, Barzaghi R, Matos AC (2014). The computation of the geoid model in the state of Sao Paulo using two methodologies and GOCE models. Boletim de Ciências Geodésicas 20(1):183-203. *https://doi.org/10.1590/s1982-21702014000100012*

Heiskanen W, Moritz H (1967). Physical Geodesy. Freeman & Co, San Francisco.

Higdon D, Swall J, Kern J (1999). Non-stationary spatial modeling, Bayesian Statistics 6(1):761-768. *https://doi.org/10.48550/arXiv.2212.08043*

ICGEM (2024). IGEM. Retrieved 24 January 2024 from *http://icgem.gfz-potsdam.de/home*

Idowu TO (2006). Prediction of gravity anomalies for geophysical exploration. FUTY Journal of the Environment 1(1):44-55. *https://doi.org/10.4314/fje.v1i1.50776*

Idowu TO, Nwilo PC, Fajemirokun FA, Ezeigbo CU (2008). Determination of optimum residual gravity anomalies for mineral exploration: A least squares collocation approach. Survey Review 40(309):294-303. *https://doi.org/10.1179/003962608x325367*

Kearsley W (1977). The estimation of mean gravity anomalies at sea from other geophysical phenomena. Ohio State University. Division of Geodetic Science. *https://kb.osu.edu/handle/1811/105257*

Kenyon SC (1998). The development by the National Imagery and Mapping Agency of a global surface gravity anomaly database for the EGM96 geopotential model and future applications. In: Forsberg R, Feissel M, Dietrich R (Eds). Geodesy on the Move. International Association of Geodesy Symposia, Vol 119. Springer, Berlin, Heidelberg. *https://doi.org/10.1007/978-3-642-72245-5_12*

Kenyon SC, Pavlis NK (1997). The development of a global gravity anomaly database used in the NIMA/GSFC geopotential model. In: Segawa J, Fujimoto H, Okubo S (Eds). Gravity, Geoid and Marine Geodesy. International

Association of Geodesy Symposia, Vol 117. Springer, Berlin, Heidelberg. *https://doi.org/10.1007/978-3-662-03482-8_63*

Knudsen P (1987). Estimation and modeling of the local empirical covariance function using gravity and satellite altimeter data. Bulletin Géodésique 61(2):145-160. *https://doi.org/10.1007/bf02521264*

Knudsen P (2005). Patching local empirical covariance functions – A problem in altimeter data processing. In: Sansò F (Ed). A Window on the Future of Geodesy. International Association of Geodesy Symposia, Vol 128. Springer, Berlin, Heidelberg. *https://doi.org/10.1007/3-540-27432-4_82*

Krarup T (1969). Contributions to the mathematical foundations of physical geodesy. Geodaetisk institut.

Krarup T (1970). Method of least squares collocation. Studia Geophysica et Geodaetica 14(2):107-109. *https://doi.org/10.1007/bf02585604*

Kwon JH, Bae T, Choi Y, Lee D, Lee Y (2005). Geodetic datum transformation to the global geocentric datum for seas and islands around Korea. Geosciences Journal 9(4):353-361. *https://doi.org/10.1007/bf02910324*

Łyszkowicz A (2010). Quasigeoid for the area of Poland computed by least squares collocation. Technical Sciences 13:147-164. *https://doi.org/10.2478/v10022-010-0014-7*

Maggi A, Migliaccio F, Reguzzoni M, Tselfe N (2007). Combination of ground gravimetry and GOCE data for local geoid determination: a simulation study. The Gravity Field of the Earth, pp. 1-6. Proceedings of the 1st International Symposium of the International Gravity Field Service, General Command of Mapping, Ankara, Turkey.

Marchenko AN, Barthelmes F, Meyer U, Schwintzer P (2002). Efficient regional geoid computations from airborne and surface gravimetry data: A case study. International Association of Geodesy Symposia 223-228. *https://doi.org/10.1007/978-3-662-04709-5_37*

Marti U (2007). Comparison of high precision geoid models in Switzerland. In: Tregoning P, Rizos C (Eds). Dynamic Planet. International Association of Geodesy Symposia, Vol 130. Springer, Berlin, Heidelberg. *https://doi.org/10.1007/978-3-540-49350-1_55*

Meissl P (1971). A study of covariance functions related to the earth's disturbing potential. Ohio State University. Division of Geodetic Science.

Milbert DG (1992). GEOID90: High-resolution geoid height model for the conterminous United States. SEG Technical Program Expanded Abstracts 1992. Society of Exploration Geophysicists, 581-584. *https://doi.org/10.1190/1.1822155*

Moritz, H. (1978). Least-squares Collocation. Moritz, H. (1978). Least-squares collocation. Reviews of Geophysics 16(3):421-430. *https://doi:10.1029/rg016i003p00421*

Odumosu JO, Nnam VC, Nwadialor IJ (2021). An assessment of spatial methods for merging terrestrial with GGM-derived gravity anomaly data. Journal of African Earth Sciences 179:104202. *https://doi.org/10.1016/j.jafrearsci.2021.104202*

Oladapo MI, Afuda FI (2017). Hydrogeophysical study of parts of Charnockite terrain of Akure southwestern Nigeria. Global Journal of Pure and Applied Sciences 23(1):107-121. *https://doi.org/10.4314/gjpas.v23i1.11*

Ono MN, Agaje AB, Onwuzuligbo CU (2017). Gravimetric Geoid Determination of Okene Town, Idah Kogi State, Nigeria. Nigerian Journal of Geodesy 1(1):113-136.

Paciorek CJ (2003). Nonstationary covariance functions for Gaussian process regression and spatial modeling. PhD Thesis, Carnegie Mellon University, Pittsburgh, Pennsylvania.

Paciorek CJ, Schervish MJ (2006). Spatial modeling using a new class of nonstationary covariance functions. Environmetrics 17(5):483-506. *https://doi.org/10.1002/env.785*

Patroba AO (2016). Assessment of EGM2008 using GPS/leveling and free-air gravity anomalies over Nairobi County and its environs. South African Journal of Geomatics 5(1):17-30. *http://dx.doi.org/10.4314/sajg.v5i1.2*

Peprah MS, Ziggah YY, Yakubu I (2017). Performance evaluation of the Earth Gravitational Model 2008 (EGM2008) A case study. South African Journal of Geomatics 6(1):47-72. *http://dx.doi.org/10.4314/sajg.v6i1.4*

Ramouz S, Afrasteh Y, Reguzzoni M, Safari A, Saadat A (2019). IRG2018: A regional geoid model for Iran using least squares collocation. Studia Geophysica et Geodaetica 63(2):191-214. *https://doi.org/10.1007/s11200-018-0116-4*

Rapp RH (1986). Global geopotential solutions. In: Sünkel H (Ed). Mathematical and Numerical Techniques in Physical Geodesy. Lecture Notes in Earth Sciences, Vol 7. Springer, Berlin, Heidelberg. *https://doi.org/10.1007/BFb0010136*

Reynolds JM (1998). An introduction to applied and environmental geophysics. John Wiley & Sons.

Risser MD, Calder CA (2015). Regression-based covariance functions for nonstationary spatial modeling. Environmetrics 26(4):284-297. *https://doi.org/10.1002/env.2336*

Risser MD, Calder CA (2017). Local likelihood estimation for covariance functions with spatially-varying parameters: The convoSPAT Package for R. Journal of Statistical Software 81(14):1-32. *https://doi.org/10.18637/jss.v081.i14*

Saadon A, El-Ashquer M, Elsaka B, El-Fiky G (2021). Determination of local gravimetric geoid model over Egypt using LSC and FFT estimation techniques based on different satellite- and ground-based datasets. Survey Review 54(384):263-273. *https://doi.org/10.1080/00396265.2021.1932148*

Sadiq M, Ahmad Z (2009). On the selection of optimal global geopotential models for geoid modeling: A case study in Pakistan. Advances in Space Research 44(5):627-639. *https://doi.org/10.1016/j.asr.2009.05.004*

Sansò F, Sideris MG (2013). Geoid Determination: Theory and Methods, Springer-Verlag, Berlin Heidelberg, *https://doi.org/10.1007/978-3-540-74700-0*

Schwarz KP, Lachapelle G (1980). Local characteristics of the gravity anomaly covariance function. Bulletin Géodésique 54(1):21-36. *https://doi.org/10.1007/bf02521093*

SNEPCO (1995). Final Report of the Gravity Survey of the Gongola Basin, Nigeria.

Tata H (2019). Determination and analysis of geoid models from observed gravity and GPS/Levelling for Akure environs, Ondo State, Nigeria. PhD Dissertation submitted to the School of Postgraduate Studies (Unpublished), Nnamdi Azikiwe University Awka, Anambra State.

Tata H (2024). Insight into the Global Gravity Models for Free-Air Gravity Estimation using Land Gravity Data. Nova Geodesia 4(2):180. *https://doi.org/10.55779/ng42180*

Tata H, Ono MN (2018). A gravimetric approach for the determination of orthometric heights in Akure environs, Ondo State, Nigeria. Journal of Environment and Earth Sciences 8(8):2224-3216.

Tata H, Ono MN, Idowu TO (2019). Development of a computational tool for the determination of the local geoid using gravimetric and GPS/Leveling approaches. Nigerian Journal of Geodesy 3(1).

Telford WM, Geldart LP, Sheriff RE (1990). Applied Geophysics. Cambridge University Press.

Timilsina S, Willberg M, Pail R (2021). Regional geoid for Nepal using least-squares collocation. Terrestrial, Atmospheric and Oceanic Sciences 32:847-856. *https://doi.org/10.3319/tao.2021.08.23.02*

Torge W (2001). Geodesy. Walter de Gruyter.

Tscherning C, Rapp RH (1974). Closed covariance expressions for gravity anomalies, geoid undulations, and deflections of the vertical are implied by the anomaly variance models. Ohio State University. Division of Geodetic Science. *https://kb.osu.edu/handle/1811/104988*

Tscherning CC (1994). Geoid determination by least-squares collocation using GRAVSOFT, Lectures Notes for the International School for the Determination and Use of the Geoid, DIIAR - Politecnico di Milano, Milano.

Tscherning CC (2001). Computation of spherical harmonic coefficients and their error estimates using least-squares collocation. Journal of Geodesy 75(1):12-18. *https://doi.org/10.1007/s001900000150*

Tscherning CC (2013). Geoid determination by 3D least-squares collocation. In: Sansò F, Sideris M (Eds). Geoid Determination. Lecture Notes in Earth System Sciences, Vol 110. Springer, Berlin, Heidelberg. *https://doi.org/10.1007/978-3-540-74700-0_7*

Tscherning CC, Forsberg R (1992). Harmonic continuation and gridding effects on geoid height prediction. Bulletin Géodésique 66:41-53. *https://doi.org/10.1007/BF00806809*

Tscherning CC, Rubek F, Forsberg R (1998). Combining airborne and ground gravity using collocation. In: Forsberg R, Feissel M, Dietrich R (Eds). Geodesy on the Move. International Association of Geodesy Symposia, Vol 119. Springer, Berlin, Heidelberg. *https://doi.org/10.1007/978-3-642-72245-5_3*

Tukka AA, Dodo JD, Ariyo TO (2016). Comparative analysis of positional results of post processed GPS survey data using Three Trimble Software Packages. Journal of Macrotrends in Applied Science (JMAS) 4(1):1-12.

You R, Hwang H (2006). Coordinate transformation between two geodetic datums of Taiwan by least-squares collocation. Journal of Surveying Engineering 132(2):64-70. *https://doi.org/10.1061/(ASCE)0733-9453(2006)132:2(64)*

Zhang K, Featherstone W (2004). Investigation of the roughness of the Australian gravity field using statistical, graphical, fractal, and Fourier power spectrum techniques. Survey Review 37(293):520-530. *https://doi.org/10.1179/sre.2004.37.293.520*